Energy Transfer between Manganese(II) and Erbium(III) in Various Fluoride Glasses*

R. REISFELD† AND E. GREENBERG

Department of Inorganic and Analytical Chemistry, Hebrew University, Jerusalem, Israel 91904

C. JACOBONI AND R. DE PAPE

Laboratoire des Fluorures et Oxyfluorures Ioniques (E. R. CNRS No. 609), Université du Maine, F-72017 Le Mans Cedex, France

AND C. K. JØRGENSEN

Département de Chimie Minérale, Analytique et Appliquée, Université de Genève, CH 1211 Geneva 4, Switzerland

The fluorescence spectra and lifetimes of fluoride glasses of molar composition $36PbF_2$, $24MnF_2$ (or ZnF_2), $35GaF_3$, 5 (or 7) $Al(PO_3)_3$, doped by ErF_3 were investigated. The emission of Mn(II) in absence of Er(III) consists of a broad band centered around 630 nm and an integrated lifetime of 1.4 msec. In the presence of Er(III) the intensity and lifetimes are decreased as a result of energy transfer to the $^4F_{9/2}$ level of Er(III). The fluorescence of Er(III) arising from $^4S_{3/2}$ at 543 nm has an integrated lifetime of 0.06 ms in the absence of Mn(II) and is decreased to 0.01 ms in the presence of Mn(II) as a result of energy transfer to Mn(II). The 666-nm luminescence of Er(III) due to $^4F_{9/2}$ emission under excitation at 370 nm ($^4G_{11/2}$) is about 20 times weaker than the 543-nm emission when Mn(II) is absent. However, in the presence of Mn(II) this emission becomes 5 times stronger than the 543-nm emission. This intensified emission has a non-exponential time dependence. The longer component corresponds to the transfer of stored energy in Mn(II) to Er(III) while the short-lived component is probably due to cascading down Er(III) → Mn(II) → Er(III) through states above the Stokes threshold of Mn(II). This interpretation is backed up by weaker 543-nm emission and stronger 630-nm broad-band emission when the mixed system is excited in one of the upper excited states, of Mn(II) at 395 nm, or of Er(III).

Introduction

Anhydrous fluorides of Pb(II), Ga(III), and Zn(II) form glasses within narrow ranges of composition (*1*). If all the Ga(III)

is replaced by Cr(III); or all the Zn(II) by Ni(II), the absorption spectra clearly indicate that these colored $3d^3$ and $3d^8$ systems are subject to local octahedral symmetry. This is also true for their aqua ions, and a large number of mixed oxides and mixed fluorides with known crystal structure (*2–4*). On the other hand, the ground state of Mn(II) has one electron in each of the *d*-like

236

orbitals, and the concomitant lack of ligand field stabilization (2, 3) provides no intrinsic propensity toward octahedral symmetry. It is true that Mn(II) aqua ions and many crystalline fluorides show $N = 6$, but several complexes of multidentate amino acid anions show $N = 7$. In fluoride glasses, where there is no sharp distinction between network formers and modifiers, large cations may have a variety of N values.

For comparison with the present spectroscopic studies, EXAFS (extended X-absorption fine-structure) of crystalline binary, ternary, and quaternary stoichiometric fluorides and of fluoride glasses (1) were performed (42). Pb(II) in such glasses seems mainly to have $N = 8$ or 9, but with a wide range of differing Pb–F distances (like in crystals) and possibly rather inequivalent sites. Mn(II), Fe(III), Zn(II), and Ga(III) seem to be octahedral. However, it cannot be excluded that $N = 6$ for Mn(II) sometimes is slightly distorted from regular octahedra, or that a part of Mn(II) has $N = 7$ or 5 through lower N values are not detected as a significant constituent. Neutron scattering (43) of glasses with the compositions $PbMnFeF_7$ and Pb_2MnFeF_9 show strong antiferromagnetic interactions in spite of the closest distance 3.6 to 3.7 Å (obtained by EXAFS) between magnetic ions suggesting corner-shared (and not edge-shared) octahedra. The Fe–F distance of 1.93 Å in such glasses is the same as found in octahedrally coordinated crystals, whereas the Mn–F distance of 2.10 Å in glasses is 0.02 Å shorter than in crystals.

Mn(II) and Fe(III) have no excited states of the configuration $3d^5$ with the same high total spin quantum number $S = \frac{5}{2}$ as the sextet ground state ^6S, and among the 252 − 6 = 246 excited states, 96 have $S = \frac{3}{2}$ (quartets). The two first absorption bands are generally rather broad (2) whereas a sharp absorption band situated somewhere in the interval between 25,300 and 21,100 cm^{-1} corresponds to some of the components of ^4G lacking ligand field influence. Comparison of this energy difference with 26,850 cm^{-1} in gaseous Mn^{+2} and 20,520 cm^{-1} in Cr^+ allows a direct evaluation of the nephelauxetic effect (2, 4) indicating weak covalent bonding with the neighbor atoms of the compound or the glass-forming medium. It is difficult to draw conclusions about the local symmetry of Mn(II) (with the exception of tetrahedral) from the position of the absorption bands below this level. Such conclusions may be drawn to some extent from the emission spectra showing a considerable Stokes shift below the first quartet. For example, salts of the tetrahedral $MnBr_4^{-2}$ show luminescence of the first quartet (5, 6) in the green with a quantum efficiency of about 1. On the other hand the red luminescence of Mn(II) in lanthanum aluminate is ascribed to octahedrally surrounded Mn(II) by oxygen ions (7). Several sites of Mn(II) were observed in calcium fluorophosphate emitting in the red (8). In oxide glasses a variety of sites is observed from the different emission spectra (9).

The absorption and fluorescence spectra of Mn(II) in phosphate, silicate, and borate glasses were treated by "ligand field" arguments by Bingham and Parke (10). These authors concluded that their silicate glasses have tetrahedral $N = 4$ and phosphate $N = 6$, whereas borate glasses contain a mixture. However, an alternative possibility, quite likely to occur also in fluoride glasses, is a heterogeneous mixture of several low-symmetry $N = 7$ or 5 and perhaps non-octahedral $N = 6$.

The high quantum yield of Mn(II) luminescence in a variety of glasses (9, 11) and crystals (12) makes them potential materials for luminescent solar concentrators provided that the low absorption bands arising from the spin-forbidden transitions will be overcome by high concentration of Mn(II). Fortunately in a number of the

glasses concentration quenching is very low (*11*). An alternative way to populate the excited state of Mn(II) would be by energy transfer from a strongly colored constituent in the glass to the lowest quartet level of Mn(II) (*13, 14*).

We have previously reported in this journal (*15, 16*) the optical transition probabilities corresponding to absorption and luminescence of Er(III) in fluoride glasses. We have also discussed the possibility (*17*) that the rare earth ions may have a variable coordination number in these glasses. Because of low vibrational frequencies of the fluoride glasses the multiphonon de-excitation of Er(III) from the excited levels (*18, 19*) is much lower than in the previously studied oxide glasses (*20, 21*) and thus the visible emission intensity is much higher.

Energy transfer for transition metal ions such as Cr(III) to M = Nd, Ho, Er, Tm, and Yb in perovskite $Y_{1-x}M_xAl_{1-y}Cr_yO_3$ (*22*) or in glasses (*23*) is an efficient way of populating the excited levels of rare earth ions (*9, 23–27*). Similar results may be obtained from energy transfer from Mn(II) to Nd, Ho, and Er in calcium phosphate glass (*28*) and Mn(II) in crystalline materials of rutile-type MnF_2 (*29*) and $RbMnF_3 \cdot Er^{3+}$ (*30*).

The purpose of the present work is to study the optical properties of Mn(II) in fluoride glasses and energy transfer between Mn(II) and Er(III) using both dynamic and static measurements.

The energy transfer probabilities and efficiencies were obtained from experimentally measured lifetimes of the donor luminescence with and without addition of the acceptor ion (dynamic measurements) and the donor luminescent quantum yield in presence of the acceptor (static method).

The efficiency of energy transfer from Mn(II) to Er(III) given by

$$\eta_{tr} = 1 - \frac{\tau_d}{\tau_d^0} \qquad [1]$$

where τ_d is the lifetime of Mn(II) in presence of Er(III).

Since the lifetimes of Mn(II) in the heavily doped fluoride glasses (with and without Er(III)) are not single exponents the average lifetimes were used

$$\tau_{av} = \frac{\int_0^\infty tI(t)dt}{\int_0^\infty I(t)dt} \qquad [2]$$

The transfer efficiency η_{tr} using the static method was obtained from formula

$$\eta_{tr} = 1 - \frac{I_d}{I_d^0} \qquad [3]$$

where I_d is the luminescence quantum efficiency of the donor ion in presence of the acceptor ion and I_d^0 is the efficiency of the donor ion in the singly doped glass.
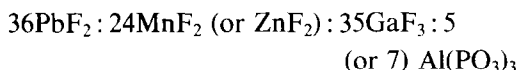
The probability of energy transfer A_{ET} can be calculated from lifetimes via

$$\frac{1}{\tau_d} = \frac{1}{\tau_0} + A_{ET} \qquad [4]$$

where τ_0 is the integrated lifetime of Mn(II) alone and τ_d of Mn(II) in the codoped glass.

Experimental

We have measured a variety of glasses of the basic composition

$36PbF_2 : 24MnF_2$ (or ZnF_2) $: 35GaF_3 : 5$
(or 7) $Al(PO_3)_3$

doped with ErF_3. They were prepared as described in Ref. (*15*) using the metal fluorides and $Al(PO_3)_3$ in the relevant proportions.

The absorption spectra were measured at room temperature on a Cary 14 spectrophotometer using an undoped Mn sample as blank or in the case of the Er-doped Zn sample relative to air.

The emission spectra were taken on a spectrofluorimeter assembled in our labora-

tory consisting of a xenon light source, two Bausch & Lomb monochromators and an EMI 9558 QB photomultiplier and were recorded at room temperature.

The decay curves of luminescence were obtained by exciting the doped glasses with a Molectron DL-200 tunable dye laser equipped with a scan control unit and pumped by a Molectron UV-400 pulsed N_2 laser. The dye used for excitation at 370 nm was Molectron PBD and at 400 nm was Molectron DPS. The signal which was normalized to the intensity of the laser pulse was fed into a PAR 162/164 boxcar averager triggered by the laser and recorded on an x–y recorder.

FIG. 1. Absorption spectrum due to manganese(II) in the glass C with molar composition 36 PbF₂ : 24 MnF₂ : 35 GaF₃ : 5 Al(PO₃)₃ : 2 LaF₃ measured at 25°C.

Results and Discussion

We have examined glasses of the following molar compositions:

C. $36PbF_2 : 24MnF_2 : 35GaF_3 : 5Al(PO_3)_3 : 2LaF_3$
D. $36PbF_2 : 24MnF_2 : 35GaF_3 : 5Al(PO_3)_3 : 2ErF_3$
E. $36PbF_2 : 24MnF_2 : 35GaF_3 : 7Al(PO_3)_3 : 0.1ErF_3$
F. $36PbF_2 : 24ZnF_2 : 35GaF_3 : 7Al(PO_3)_3 : 0.1ErF_3$

and compared them with two glasses (15) previously studied:

A. $46PbF_2 : 22MnF_2 : 30GaF_3 : 2LaF_3$
B. $46PbF_2 : 22ZnF_2 : 30GaF_3 : 2LaF_3$

to which 2 wt% ErF_3 had been added.

The aluminum metaphosphate in samples C to F assists efficiently in obtaining stable vitreous phases, but its addition cannot be neglected as it has quite a striking effect on the lifetimes of the Er(III) levels $^4S_{3/2}$ and $^4F_{9/2}$ being, respectively, 3 and 4 times shorter in glass F than in glass B. See Table IV of Ref. (15).

Since the stoichiometric ratio oxygen/fluorine is $45/231 = 0.195$ in glasses C and D, the much higher P–O vibrational frequency may be responsible for this higher multiphonon relaxation of Er(III) in the glass in which Er may be closer to the O atoms of the P–O groups (19).
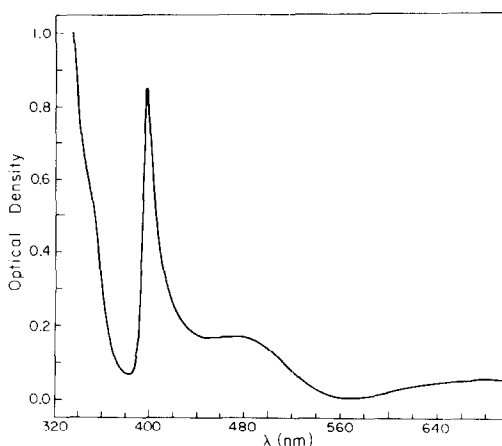
1. Manganese

The absorption spectrum of C containing Mn(II) without Er(III) is given in Fig. 1. The steeply increasing absorption in the uv is due (5) to Pb(II). The uncharacteristic slope of absorption starting at 560 nm and developing into one flat maximum at 480 nm before the sharp maximum at 398 nm $(25,100 cm^{-1})$ would not occur for a single octahedral site, expected to show two absorption bands of comparable width and intensity (2, 6, 31) around 530 and 440 nm. There is a slight possibility that the spectrum could be the superposition of octahedral and relatively more absorbing, tetrahedral sites, but this seems unlikely in view of the small ionic radius of F^- favoring high N values. The observed spectrum (Fig. 1) is at least compatible with a multitude of different low-symmetry sites tending (2, 6) to have the narrow ^4G band decreasing much more abruptly toward higher wavenumbers than the hyperbolic slope down to the lower quartets. This is readily rationalized even for a single site by it no longer being the case (as in cubic symmetries) that a third of the 36 states of ^4G essentially coincide. The situation is not made more clear-cut by the
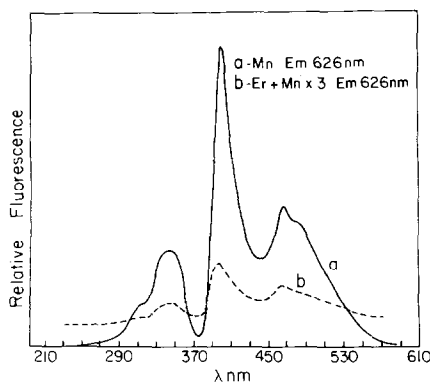
FIG. 2. Excitation spectra of manganese(II) emission at 626 nm. Curve (a): glass C. Curve (b): glass D where the 2 mole% LaF₃ of C is replaced by ErF₃. Measured at 27°C.

strong variation of emission maxima of antiferromagnetic halide-bridged MnXMn in salts (32) and of the fluorescence spectrum as a function of the concentration, 1.3 to 25 molar% of Mn(II) in a magnesium zinc phosphate glass (9).

The aqua ions and many other complexes of Mn(II) are octahedral (6, 31) and Mn halides such as $MnBr_4^{-2}$ are tetrahedral. However, because of the large ionic radius of Mn(II) and lack of ligand field stabilization (2, 3) there is no intrinsic propensity toward either octahedral or tetrahedral symmetry. Actually the monaqua ethylenediaminetetraacetate and other Mn(II) complexes of multidentate amino acids show the coordination number of $N = 7$ (33). There is a small point of similarity between Mn(II) and the lanthanides by a sharp absorption band situated in the interval between 25,300 and 21,100 cm⁻¹ representing some of the states of ⁴G lacking "ligand field" influences like ⁶S.

The excitation spectrum of the Mn(II) broad-band emission at 626 nm is presented in Fig. 2 where curve (a) belongs to excitation of C and curve (b) to D containing 2 molar% ErF₃. It should be noted that the sensitivity of curve (b) is increased by a fac-

tor of 3.3 indicating decreased luminescence of Mn(II) in the presence of Er(III) as a result of energy transfer (mainly to ⁴F₉/₂) from Mn(II) to Er(III).

The emission spectrum of Mn(II) in glass C under excitation in the narrow ⁴G peak at 395 nm is given in Fig. 3, curve (a) showing a broad maximum at 626 nm corresponding to emission from the lowest quartet to the ⁶S ground state. This band is quite similar to the 600-nm fluorescence in vitreous $K_3P_7O_{19}$ (10). The decay of C emission is non-exponential but can be roughly described by two superposed lifetimes, 1.06 and 1.82 msec, with the integrated (averaged) $\tau = 1.45$ msec. Glass D also shows two decay times, 0.15 and 0.43 msec, with integrated $\tau = 0.34$ msec.

From the luminescence spectrum of Mn(II) in fluoride glasses (Fig. 3) one can see that there is no emission from the tetrahedral sites which means that either the tetrahedral sites are absent or that there may be energy transfer from the tetrahedral sites, which should emit in the green, to the octahedrally like sites emitting in the red.
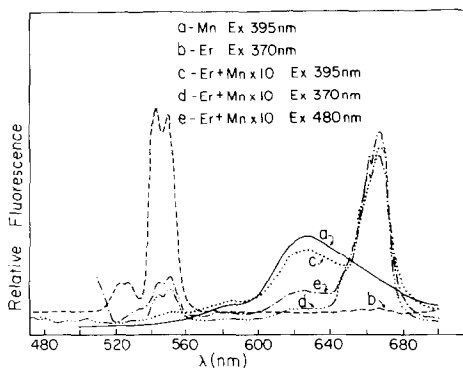

FIG. 3. Fluorescence spectra of various glasses. Curve (a): Glass C excited at the Mn(II) peak at 395 nm. Curve (b): Glass F excited at the Er(III) peak at 370 nm. Curve (c): Glass D excited at the Mn(II) peak at 395 nm. Curve (d): Glass D excited at the Er(III) peak at 370 nm. Curve (e): Glass D excited at the Mn(II) peak at 480 nm. The sensitivity used for curves (c), (d), and (e) are all 10 times higher than the sensitivity used for curves (a) and (b). Measured at 27°C.
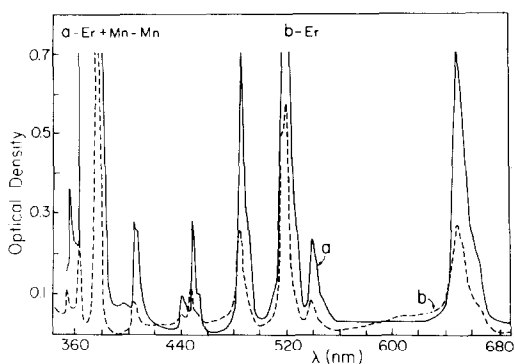
FIG. 4. Absorption spectra due to erbium(III). Curve (a): Glass D measured against the erbium-free glass C as reference, with the intention of compensating the absorption due to manganese. Dashed curve (b): Glass F containing no manganese. Measured at 25°C.

Since the lifetimes of Mn(II) alone are non-exponential we conclude that the different Mn(II) sites do not all communicate. This arises from the fact that in the case of fast diffusion of energy between the various sites the lifetime should be exponential (34).

When glass D is excited at 480 nm (avoiding Er(III) peaks, and a representative wavelength for Mn(II) absorption in glass C in Fig. 1) the intensity of 666 nm is about 5 times higher than the 543-nm emission, as seen in Fig. 3, curve (e).

The strong variation of the emission spectrum (9) as a function of Mn(II) concentration known from the literature may not only be due to a modified manifold of sites but also to efficient energy transfer from one Mn(II) to another having its lowest quartet level at lower energy, or at most, at a few kT higher energy. A superposition of these two mechanisms occurs in antiferromagnetically coupled pairs of Mn(II) bridged by one or a few fluoride anions, approaching the situation in Cl₃WCl₃WCl₃⁻³. Extensive energy transfer between different sites on Mn(II) in crystalline materials, such as in rutile-type

MnF₂ (29, 35, 36) where $N = 6$ for Mn(II) and hence $N = 3$ for F⁻, is known. Actually the influence of crystalline defects and of ppm impurities of Mg(II) is so strong that there was difficulty in detecting the intrinsic Stokes threshold for the very long-lived quartet. The experimental work is slightly easier to interpret in the cubic erbium-containing perovskites RbMnF₃ (30) and RbMgF₃ (37) where $N = 6$ in a regular octahedron constituting alternating FMn FMnFMn . . . on each Cartesian axis. Quite strong changes of fluorescence spectra are found when cooling below the Néel temperature.

2. Erbium

The absorption spectra of Er(III) in our new fluoride glasses are shown in Fig. 4 where curve (a) is the difference in absorption between glass D and the erbium-free glass C. Curve (b) is the absorption of glass F containing ZnF₂ in place of MnF₂. There is no perceptible difference between the shape, half-width, and positions of Er(III) bands in the two curves. Such behavior was noted previously (15) for glasses A and B though somewhat enhanced Er(III) intensi-
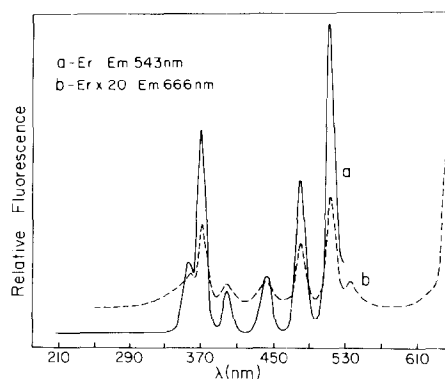

FIG. 5. Excitation spectra of erbium(III) emission in the manganese-free glass F. The full curve (a) is monitored for fluorescence at 543 nm. The dashed curve (b) is monitored at 666 nm, using 20 times higher sensitivity than for curve (a). Measured at 27°C.

ties were noted below 700 nm for manganese-containing A.

The excitation spectrum of Er(III) in glass F for the 543-nm emission, $^4S_{3/2} \rightarrow$ $^4I_{15/2}$, is shown in Fig. 5, curve (a), whereas curve (b) is monitored at 666-nm emission due to $^4F_{9/2} \rightarrow$ $^4I_{15/2}$. The sensitivity for curve (b) is about 20 times higher than in curve (a) meaning that the 666-nm red emission is negligible compared to the 543-nm green emission in the erbium-only glass F.

The emission spectrum of Er(III) alone in glass F excited in the narrow absorption band at 370 nm, $^4G_{11/2}$, is shown in Fig. 3, curve (b). A weak emission band is observed at 525 nm, $^2H_{11/2} \rightarrow$ $^4I_{15/2}$ and a much stronger emission at 543 nm, $^4S_{3/2} \rightarrow$ $^4I_{15/2}$. The band at 666 nm is exceedingly weak, cf. Fig. 5.

The integrated lifetime of 0.1% ErF_3 alone (F) is 0.098 msec for 543-nm emission and 0.084 msec for 666 nm. The lifetime of 2% ErF_3 with Mn(II) in D is 0.009 msec for 543 nm and about 0.025 msec for 666-nm fluorescence. We did not have a glass of Er(III) alone at the higher concentration but there is little doubt that the values would be intermediate between F and D. Glass B without $Al(PO_3)_3$ (15) had $\tau = 0.29$ msec for $^4S_{3/2} \rightarrow$ $^4I_{15/2}$ and 0.35 msec for $^4F_{9/2}$ $\rightarrow$ $^4I_{15/2}$ (about 3 to 4 times longer than F despite the 20 times higher erbium concentration).

3. Energy Transfer between Manganese and Erbium

The energy transfer from Mn(II) to Er(III) can be seen in the emission spectrum of the composite glass D given in Fig. 3 curve (c). This glass is excited at 395 nm at the manganese absorption peak. The curve consists of a broad emission band peaking at 626 nm due to the lowest-lying quartet state of Mn(II) and the narrow structural 666-nm band of Er(III) arising from the transition $^4F_{9/2}$ to $^4I_{11/2}$. The intensity of the Mn(II) emission is decreased by
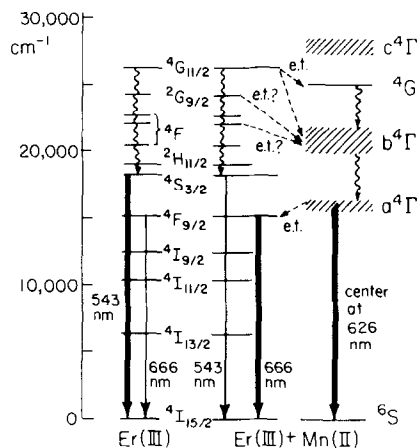

FIG. 6. Major radiative (thick vertical arrows for strong fluorescence) and non-radiative (wavy arrows) processes in a fluoride glass doped with Er(III) alone (to the left) or both Er(III) and Mn(II) (to the right). The symbols of atomic spectra indicate J-levels of the $4f^{11}$ system erbium(III) and the terms ^6S and ^4G of $3d^5$ manganese(II). The group-theoretical symbols $^4\Gamma$ indicate quartet states belonging to Mn(II) on (probably inequivalent) sites of undetermined point-group symmetry. The effects of intermediate coupling are quite strong in higher levels of Er(III) and the highest squared amplitude (44) is for $^2G_{9/2}$ (though it is only 34% in the next-highest level on the figure. We sometimes (15, 16) have called it $^2H_{9/2}$ (21% (44)). Energy transfer (e.t.) is shown as stipled slopes. The two question marks refer to cases, where energy transfer from excited $^4G_{11/2}$ to Mn(II) may go through various intermediate states.

a factor of 10 as compared to the emission of Mn(II) in the Mn-only glass as a result of energy transfer to the $^4F_{9/2}$ state of Er(III). The Er(III) emission at 543 nm arising from the transition $^4S_{3/2} \rightarrow$ $^4I_{15/2}$ is almost totally absent (curve (c)) unlike in curve (b).

The energy transfer scheme is presented in Fig. 6 in which the levels of Mn(II) and Er(III) are designated. In this figure the thick arrows indicate fluorescence, the wavy lines the nonradiative relaxations, and the broken lines designate energy transfer.

The probability of this energy transfer between Mn(II) and 2 mole% Er(III) is 2300 sec^{-1} as calculated from formula [4] and the
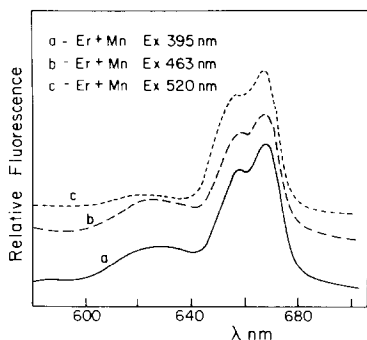
FIG. 7. Emission spectra of Mn(II) and Er(III) in glass D under (a): excitation at 395 nm, (b): excitation at 463 nm, and (c): excitation at 520 nm.

experimentally measured lifetimes. The energy transfer efficiency from the lowest quartet of Mn(II) to $^4F_{9/2}$ in glass D is 0.77 to be compared with 0.86 obtained by Parke and Cole (28) for $(29.85 - 0.3x)Na_2O : (69.5 - 0.7x)SiO_2 : 0.5MnO : xEr_2O_3$ for $x = 2$, 0.73 for $x = 1$, and 0.42 for $x = 0.5$. In the latter glasses the manganese concentration is some 50 times lower than in our fluoride glasses.

Figure 3, curve (d), shows the emission of the same glass D excited at 370 nm ($^4G_{11/2}$ of Er(III)). We observe a much stronger emission at 666 nm than at 543 nm and a rather moderate contribution of Mn(II) at 626 nm. A similar picture is obtained when glass D is excited at 395 nm, excitation of Mn(II) Fig. 7 (curve (a)), a 463 nm of Mn(II) + Er(III) (curve (b)) and 520 nm of Er(III) (curve (c)). This demonstrates energy transfer from Er(III) to Mn(II) in the opposite direction of curve (c) and an equilibrium between the population of the lowest quartet state of Mn(II) and the $^4F_{9/2}$ state of Er(III). The most plausible explanation is that excitation in the narrow ^4G band of Mn(II) rapidly populates the lowest quartet level nonradiatively. The latter level transfers energy to $^4F_{9/2}$ of Er(III). Since the Stokes threshold of this level is too low to permit population of $^4S_{3/2}$ the 543-nm emis-

sion is absent. On the other hand the $^4G_{11/2}$ and lower lying levels of Er(III) have smaller probabilities of decay to the lower $^2H_{11/2}$ and $^4S_{3/2}$ levels of Er(III) than to transfer energy to relatively high-lying Mn(II) quartet levels (on distorted potential surfaces in $(3n - 5)$ dimensions for n nuclei) which in turn can transfer energy back to the $^4F_{9/2}$ of Er(III). In other words the 666-nm narrow band emitted by glass D subsequent to $^4G_{11/2}$ or other excitation of Er(III) goes through the nonradiative channels $^4G_{11/2}$ (Er) $\rightarrow$ higher quartets (Mn) $\rightarrow$ lowest quartet (Mn) $\rightarrow$ $^4F_{9/2}$ (Er).

This mutual energy transfer and cascading down to $^4F_{9/2}$ as seen in Fig. 7 is also backed up by the decay curve of $^4F_{9/2}$ emission at 666 nm in the codoped glass D. The short-lived part of the decay curve has τ shortened by the presence of manganese to 0.025 msec from the value 0.08 msec found for F. The long-lived part of the decay curve is much weaker but lasts so much longer that the area has the same order of magnitude corresponding to energy transferred back to $^4F_{9/2}$ after storage in the long-lived Mn(II). It must be admitted that the long-lived part of the decay curve still has a much smaller τ (it is not exponential to any good approximation but is above 0.2 msec) than 1.4 msec of glass C. Besides the obvious shortening due to energy transfer to $^4F_{9/2}$ it also seems that glass D has some anomalous short-lived Mn(II) sites detected by this measurement. Such sites may have short MnFEr distances.

Extensive energy transfer from Mn(II) to Nd(III) is nearly one-dimensional $CsMnBr_3$ crystals (38) and between Mn(II) and Er(III) in $RbMnF_3$ crystals (30) has been attributed to migration of energy between the chain of manganese ions followed by transfer to the rare earth ion. In our case where the system is disordered the energy may be transferred by any manganese ion in the vicinity of an erbium ion. Since the magnitude of the transfer efficiency of energy in

this case is similar to the transfer efficiencies of post-transition ions to the rare earth ions (Ref. (*13*), Table I and Ref. 23, Table I) we believe that the transfer mechanism is mainly dipole–dipole assisted by the phonons of the glass-forming medium.

Acknowledgments

References

1. J. P. MIRANDAY, C. JACOBONI, AND R. DE PAPE, *J. Non-Cryst. Solids* **43**, 393 (1981).

2. C. K. JØRGENSEN, "Absorption Spectra and Chemical Bonding in Complexes," Pergamon, Oxford (1962).

3. C. K. JØRGENSEN, "Modern Aspects of Ligand Field Theory," North-Holland, Amsterdam (1971).

4. C. K. JØRGENSEN, "Oxidation Numbers and Oxidation States," Springer-Verlag, Berlin (1969).

5. R. REISFELD AND C. K. JØRGENSEN, "Lasers and Excited States of Rare Earths," Springer-Verlag, Berlin (1977).

6. C. K. JØRGENSEN, *Acta Chem. Scand.* **11**, 53 (1957).

7. A. L. N. STEVELS, *J. Lumin.* **20**, 99 (1979).

8. F. M. RYAN, R. C. OHLMANN, J. MURPHY, R. MAZELSKY, G. R. WAGNER, AND R. W. WARREN, *Phys. Rev. B* **2**, 2341 (1970).

9. R. REISFELD AND C. K. JØRGENSEN, *Struct. Bonding* **49**, 1 (1982).

10. K. BINGHAM AND S. PARKE, *Phys. Chem. Glasses* **6**, 224 (1965).

11. A. KISILEV, R. REISFELD, AND H. TZEHOVAL, Fourth Int'l Conf. on Photochem. Conversion and Storage of Solar Energy, Book of Abstracts, 299 (1982).

12. J. DANKO, D. PACHECO, AND B. DIBARTOLO, *J. Lumin.* **28**, 27 (1983).

13. R. REISFELD, *Struct. Bonding* **30**, 65 (1976).

14. R. C. POWELL AND G. BLASSE, *Struct. Bonding* **42**, 43 (1980).

15. R. REISFELD, G. KATZ, N. SPECTOR, C. K. JØRGENSEN, C. JACOBONI, AND R. DE PAPE, *J. Solid State Chem.* **41**, 253 (1982).

16. R. REISFELD, G. KATZ, C. JACOBONI, R. DE PAPE, M. G. DREXHAGE, R. N. BROWN, AND C. K. JØRGENSEN, *J. Solid State Chem.* **48**, 323 (1983).

17. C. K. JØRGENSEN AND R. REISFELD, *Top. Curr. Chem.* **100**, 127 (1982).

18. R. REISFELD, *Struct. Bonding* **13**, 53 (1973).

19. R. REISFELD, *Struct. Bonding* **22**, 123 (1975).

20. R. REISFELD, L. BOEHM, Y. ECKSTEIN, AND N. LIEBLICH, *J. Lumin.* **10**, 193 (1975).

21. R. REISFELD AND Y. ECKSTEIN, *J. Chem. Phys.* **63**, 4001 (1975).

22. M. J. WEBER, *J. Appl. Phys.* **44**, 4058 (1973).

23. R. REISFELD, "Energy Transfer between Inorganic Ions in Glasses," Erice Summer School, June 1983.

24. L. J. ANDREWS, A. LEMPICKI, AND B. C. McCOLLUM, *Chem. Phys. Lett.* **74**, 404 (1980).

25. L. J. ANDREWS, A. LEMPICKI, AND B. C. McCOLLUM, *J. Chem. Phys.* **74**, 5526 (1981).

26. T. HÄRIG, G. HUBER, AND I. A. SHCHERBAKOV, *J. Appl. Phys.* **52**, 4450 (1981).

27. A. KISILEV AND R. REISFELD, Solar Energy, in press.

28. S. PARKE AND E. COLE, *Phys. Chem. Glasses* **12**, 125 (1971).

29. J. M. FLAHERTY AND B. DIBARTOLO, *in* "Colloque CNRS No. 255, Lyon, 1976" (F. Gaume, Ed.), p. 191, CNRS, Paris (1977).

30. M. V. IVERSON AND W. A. SIBLEY, *Phys. Rev. B* **21**, 2522 (1980).

31. L. E. ORGEL, *J. Chem. Phys.* **23**, 1824 and 1958 (1955).

32. D. OELKRUG *et al., Ber. Bunsenges.* **80**, 436 and 441 (1976).

33. G. H. COHEN AND J. L. HOARD, *J. Amer. Chem. Soc.* **86**, 2749 (1964).

34. R. REISFELD, *in* "Radiationless Processes" (B. DiBartolo and V. Goldberg, Eds.), p. 489, Plenum, New York (1980).

35. J. HEGARTY AND G. F. IMBUSCH, *in* "Colloque CNRS No. 255, Lyon, 1976" (F. Gaume, Ed.), p. 199, CNRS, Paris (1977).

36. J. M. FLAHERTY AND B. DIBARTOLO, *Phys. Rev. B* **8**, 5232 (1973).

37. M. D. SHINN, J. C. WINDSCHEIF, D. K. SARDAR, AND W. A. SIBLEY, *Phys. Rev. B* **26**, 2371 (1982).

38. G. L. McPHERSON AND A. H. FRANCIS, *Phys. Rev. Lett.* **41**, 1681 (1978).

39. B. A. WILSON, W. M. YEN, J. HEGARTY AND G. F. IMBUSCH, *Phys. Rev. B* **19**, 4238 (1979).

40. R. L. GREENE, D. D. SELL, R. S. FEIGELSON, G. F. IMBUSCH, AND H. J. GUGGENHEIM, *Phys. Rev.* **171**, 600 (1968).

41. U. KAMBLI-KALLEN, "Energietransfer in den Alkalimanganhalogeniden CsMnBr₃, CsMnCl₃, RbMnCl₃ und Rb₂MnCl₄," dissertation, University of Bern (1983).

42. A. LE BAIL, C. JACOBONI, AND R. DE PAPE, *J. Solid State Chem.*, submitted for publication.

43. A. LE BAIL, C. JACOBONI, AND R. DE PAPE, *J. Phys. Colloq. C9.* **43**, 677 (1982); *J. Solid State Chem.* **48**, 168 (1983).

44. B. G. WYBOURNE, *J. Chem. Phys.* **34**, 279 (1961).